

Thresholding Values and Fuzzy Logic Fusion in Visualisation of Gas-Oil-Water Horizontal Flow using Dual-Modality Electrical Tomography

Qiang Wang, Mi Wang*

School of Chemical and Process Engineering, University of Leeds, Leeds, UK

*Email: m.wang@leeds.ac.uk

ABSTRACT

Two different data fusion approaches, namely the thresholding and fuzzy logic-based data fusion, have been proposed to address the challenges in the use of dual-modality electrical tomography (ERT-ECT) for visualising gas-oil-water horizontal flow. This paper introduces both methods and compares their performance on visualisation of six common flow regimes in horizontal pipe flow of industrial-scale multiphase flow testing facility, including stratified flow, wavy stratified flow, slug flow, plug flow, bubbly flow, and annular flow. The paper reports experimental results which reveals specific advantages and limitations of each approaches. Overall, the threshold-based approach, including data fusion and phase decomposition, is simple at the aspects of understanding and implementation. It is fast and requires little computing resources, and therefore suitable for online purpose. The selection of thresholding values, however, have obvious impacts on the results since the determination of the thresholding values requires prior knowledge, which could be affected by site and operation factors. In contrast, fuzzy logic-based method is much more complicated than the thresholding method since it utilises the fuzzy inference system and decision tree to perform the fusion and carry out the decomposition respectively. Accordingly, this advanced method costs more time and computing resources to derive the final results. However, it does not need prior knowledge on threshold values and hence is insensitive to the changes of membership functions, which makes this method more robust than the thresholding value method. In addition, the results from visualisation of industrial flows demonstrated the fuzzy logic fusion method has a better performance on reporting phase boundaries.

Keywords dual-modality electrical tomography, gas-oil-water horizontal flow, multiphase flow visualisation, multi-dimensional data fusion, thresholding fusion, fuzzy logic fusion

Industrial Application Oil and Gas

1 INTRODUCTION

Gas-oil-water three-phase flow is a common physical phenomenon in many industrial sectors, e.g. gas&oil production. When fluid is extracted from a well, it generally contains time-varying ratios of gas, oil, and water. Due to the unpredictable and complex interactions between the phases, it is extremely challenging to understand such phenomenon. Process tomography as a non-intrusive approach has been intensively studied and applied to multiphase flow visualisation and measurement (Wang, 2015). Due to the incapability of single-modality tomography on characterising the flow containing more than two phases, multi-modality tomographic systems have been proposed to deal with three-phase flow (Hoyle et al., 2001, Qiu et al., 2007, Sun and Yang, 2015). The majority of the efforts have been made on the hardware and reconstruction algorithms, but very limited investigations have been conducted on the method of data fusion based on specific characteristics of multiphase flows.

Data/image fusion has been intensively investigated in the past a few decades, and a variety of approaches have been proposed in many areas, e.g. medical imaging and multi-sensor fusion. It seems trivial to migrate those mature approaches to multi-modality process tomography with little effort. This, however, is not the case due to the unique characteristics of multi-modality process tomography and multiphase flow. In general, multi-phase flow visualisation and measurement requires not only spatial information but also temporal contents to reflect flow dynamics, e.g. flow regimes. In addition, both qualitative (e.g. images) and quantitative (e.g. phase concentrations) information is needed for

multiphase flow characterisation. In case of electrical tomography, the data fusion becomes more complicated primarily because of the low spatial resolution.

So far, the primary approach in process tomography-based three-phase flow visualisation relies on the thresholding basis, i.e. using threshold values to binarize each tomograms from different modalities, e.g. the methods reported by Qiu et al. (2007), and Sun and Yang, (2015). Unfortunately, there are commonly shared limitations existed in these threshold-based approach, e.g. their capabilities were evaluated from limited flow conditions. Few advanced algorithms have been proposed, like fuzzy clustering for two-phase flow with ERT-ECT (Yue et al., 2013), and fuzzy logic for ECT and Ultrasound tomography (Pusppanathan et al., 2014). However, their applicability to ERT-ECT-based three-phase flow visualisation did not be reported.

The focus of this paper is to address the challenges in the use of dual-modality electrical tomography for quantifying and qualifying gas-oil-water three-phase horizontal flow. Two different approaches have been investigated (Wang 2017). One of them is built upon the conventional threshold-based the other employs fuzzy logic with decision tree. Both methods have been evaluated using the data acquired from a dual-modality electrical tomography (ERT-ECT) from an industrial-scale flow testing facility at the National Engineering Laboratory (NEL). The results on typical flow regimes are reported in the paper, which covers the six common flow regimes, i.e. stratified flow, wavy stratified flow, plug flow, slug flow, annular flow, and bubbly flow.

In this paper, both approaches are briefly introduced, and their performance on the six common flow regimes will be compared based on experimental data acquired from a flow facility with a commercial ERT-ECT systems.

2 METHODOLOGIES

2.1 Data pre-processing

When using ERT-ECT systems to visualise gas-oil-water horizontal flow, there are several inherent challenges. Due to the differences in image format and data sampling rate of the engaged modalities and image reconstruction algorithms, the resultant electrical tomograms represent distributions of different electrical properties, with different spatial and temporal resolutions. Therefore, how to integrate the tomograms containing different spatial and temporal information is the first challenges to be addressed. In addition, due to the nature of multiphase flow, cross-sectional images may not be enough to reflect flow dynamics, e.g. flow regimes, and hence alternative representations need to be figured out so that more flow dynamics information can be conveyed. Another challenging issue is the low spatial resolution of electrical tomograms for visualising multiphase flow, e.g. blurred boundaries between bubbles and liquid. This limitation affects the application of the image fusion algorithms utilising image features and visible objects, which means only pixel-level fusion methods are applicable to electrical tomograms.

In order to convey more flow dynamics information, the cross-sectional tomograms are firstly stacked along pipe axis. That is, axially-stacked tomograms are generated from two sets of original tomograms to provide both spatial and temporal information of the flow under investigation. Afterwards, two axially-stacked tomograms are registered from their own coordination systems to a common coordination system so that every corresponding pixels in the tomograms represents exactly the same physical phenomenon in both spatial and temporal terms.

In this study, commercial ERT (V5R) and ECT (M3C) were utilised for the experiments. The ERT features with the sampling speed at 62.5 frame per second (fps), whereas the ECT works at the speed of 12.5 fps. In addition, due to the difference between the reconstruction algorithms, the reconstructed cross-sectional tomograms are with different mesh definitions, i.e. ERT tomograms are 20*20 whereas ECT tomograms are 32*32. Therefore, the tomograms have to be registered at spatial and temporal axes. Due to the simplicity in theory and implementation terms, linear interpolation was chosen for the registration.

2.2 Data fusion

After the transformation and registration, the resultant tomograms are ready to allow pixel-level fusion algorithms to be performed. Based on the unique characteristics in this area, two algorithms were developed to overcome the challenges, including the threshold-based fusion and fuzzy logic with decision tree-based fusion. The principles behind two approaches are briefly introduced in the following sections.

2.2.1 Threshold-based data fusion

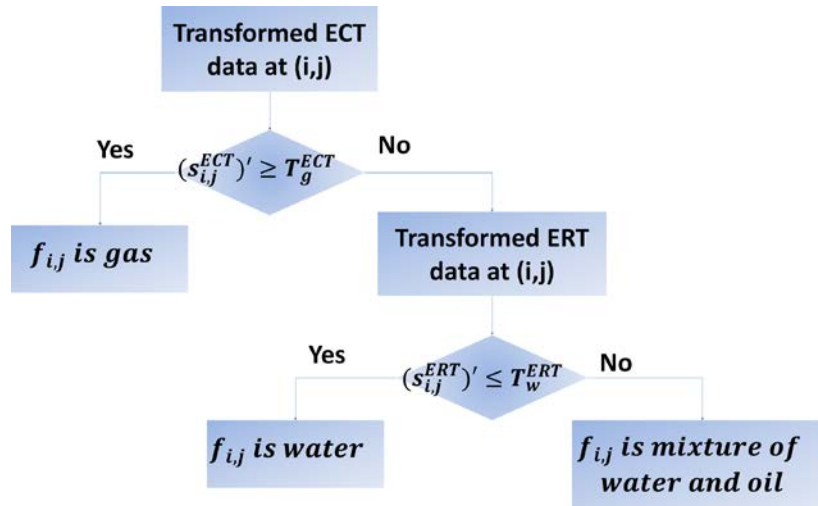


Figure 1: Data flow of the threshold-based fusion (Wang et al. 2017).

The principle behind the threshold-based fusion is to use ECT to distinguish gas from water and oil, and use ERT to distinguish water from gas and oil. The over procedure of the fusion is depicted in Figure 1. In principle, the concentration $s_{i,j}^{ECT}$ of a pixel at (i, j) in the processed ECT tomogram is firstly compared with a threshold T_g^{ECT} . If the pixel concentration is beyond the threshold T_g^{ECT} , the pixel is considered to be fully occupied by gas, or otherwise it contains oil and/or water. In later case, the concentration $s_{i,j}^{ERT}$ of the processed ERT tomogram at the corresponding pixel (i, j) is compared to another threshold value T_w^{ERT} . If the value is below T_w^{ERT} , the corresponding pixel is filled with water, or otherwise it contains a mixture of oil and water.

2.2.2 Fuzzy logic with decision tree-based data fusion

The major issue of conventional threshold-based fusion is whether the threshold values is not trivial as it may be affected by many factors, e.g. hardware, image reconstruction algorithms, and flow conditions, and so on. To enhance the visibility, assumptions are made to describe the general contribution of individual phase to tomograms Taking account of the threshold in electrical tomograms of each modality (i.e. ERT or ECT) is usually taken at middle of a full concentration range, i.e. 50% of the full concentration range [0%, 100%] can be divided into four sub-ranges, namely low, low-mid, mid-high, and high concentration sections. Considering the widely accepted overall uncertainty around 5% of local disperse phase concentration imaged with electrical tomography, the concentration at the pixel is assumed only to be filled with water for ERT, or a liquid (water-oil mixture) for ECT as the pixel concentration is less than 5%. In the mid-low concentration section, the flow assumed to be a mixture of gas, oil, and water for both ERT and ECT imaging. In the high concentration section, the flow is assumed only a gas-oil mixture (low conductivity) for ERT, but gas (low permittivity) for ECT. In the mid-high section where the threshold fell in, the flow can be those in low-mid and high sections. Figure 2 illustrates how the four concentration sub-ranges depict the possible fluid phase components form the method to fuse ERT and ECT images.

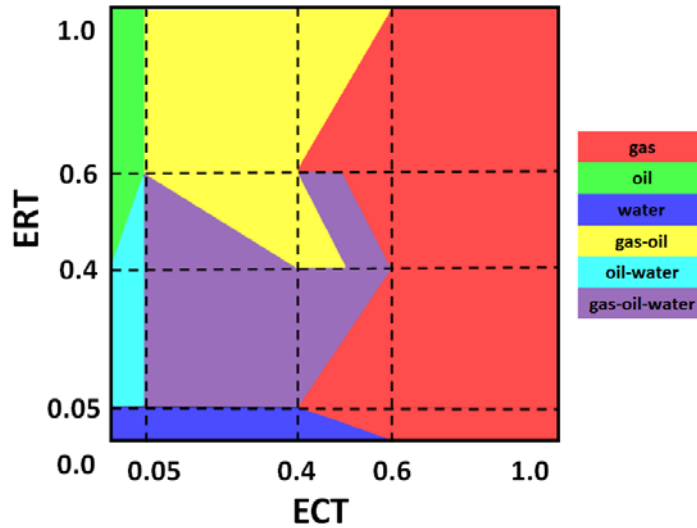


Figure 2: Possible component distribution for ERT and ECT concentration tomograms.

Following above fundamental principle, a fuzzy inference system (FIS) can be constructed to determine possible combinations of gas, oil, and water phase, as well as the probability of each combination if there are more than one combinations. With the combinations and the probability assumption, a mixture can be decomposed into individual phase and concentration values of each phase can be estimated. Overall, the FIS for our purpose has two inputs from ECT and ERT images and two outputs for gas+oil and oil+water. The inputs are fuzzified firstly using membership functions to obtain corresponding membership degrees. Afterwards, 16 pre-defined rules are identified as illustrated in Figure 2 and evaluated according to the membership degrees, of which the results are aggregated for later process. Finally, the aggregation is defuzzified to a crisp value as a basis for the decomposition and estimation. Based on the defuzzified results, a decision tree is applied to derive pixel concentrations of individual phases. Interested readers can refer to Wang (2017) for technical details.

2.3 Data post-processing

Data post-processing is to decompose individual phases and derive their pixel concentrations, and finally display decomposed results with conventional colour mapping. Let $P = \{p_{x,y} \mid x \in \{1, 2, L, N\}, y \in \{1, 2, L, Q\}\}$ denote the decomposed pixel concentration, where N and Q are the dimensions of the fused tomograms. Since for every pixel $p_{x,y}$ in the fused result F , phase composition can be described as:

$$p_{x,y} = (\alpha_{x,y}^g, \alpha_{x,y}^o, \alpha_{x,y}^w); \alpha_{x,y}^x \in [0, 1]; \quad (1)$$

where $\alpha_{x,y}^x$ represents local pixel concentration of the phase x , which satisfies:

$$\alpha_{x,y}^g + \alpha_{x,y}^o + \alpha_{x,y}^w = 1 \quad (2)$$

Based on Equation 1 and Equation 2 and the decomposition procedure (Wang et al., 2017) for the threshold-based approach and the fuzzy logic with decision tree based approach (Wang 2017), the decomposed pixel concentration P can be derived.

A predominant visualisation approach for scalar data is colour mapping, i.e. transferring scalar data to different colours in line with a lookup table. A colour space $C = \{c_{x,y} \mid x \in \{1, 2, L, N\}, y \in \{1, 2, L, Q\}\}$ for the fused tomogram can be defined as:

$$c_{x,y} = (r_{x,y}, g_{x,y}, b_{x,y}), r_{x,y}, g_{x,y}, b_{x,y} \in [0, 255] \quad (3)$$

where r , g , and b are the fundamental colors in RGB space, i.e. red, green, and blue. Accordingly, a transfer function T can be defined using matrix multiplication:

$$[r_{x,y}, g_{x,y}, b_{x,y}] = [\alpha_{x,y}^g, \alpha_{x,y}^o, \alpha_{x,y}^w] \begin{bmatrix} 255 & 0 & 0 \\ 0 & 255 & 0 \\ 0 & 0 & 255 \end{bmatrix} \quad (4)$$

3 EVALUATION

3.1 Experimental setup

Experiments were carried out on gas-oil-water flow in industry-scale flow facilities in TUV NEL UK, of which its multiphase flow loop is a three component flow facility featuring oil, water and gas. A graphical representation of the flow facility is shown in Figure 3. For measurement purposes, Paraflex (HT9) oil is used alongside substitute salt water (Magnesium Sulphate MgSO₄) and a dry gas (Nitrogen) is injected externally via a pressurised storage tank.. Different Water-in-Liquid Ratio (WLR) and Gas Volume Fraction (GVF) were combined in order to produce common flow regimes in horizontal pipe. The selected testing matrix for the evaluation of the proposed imaging approach is shown as Table 1.

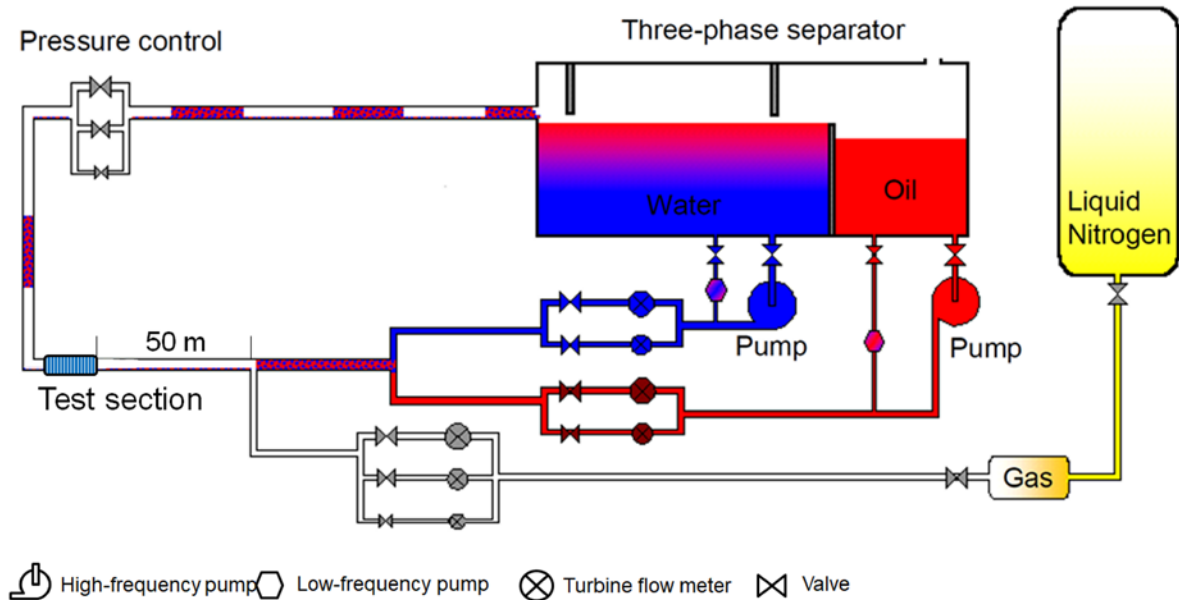


Figure 3: Schematic of NEL Multiphase Flow Facility (Millington, 2016).

Table 1: Selected flow conditions for evaluating the proposed approach.

	WLR(%)	GVF(%)
Stratified flow	50	60
Wavy stratified flow	75	70
Slug flow	75	42
Plug flow	75	5
Annular flow	90	92
Bubbly flow	90	35

3.2 Data fusion results

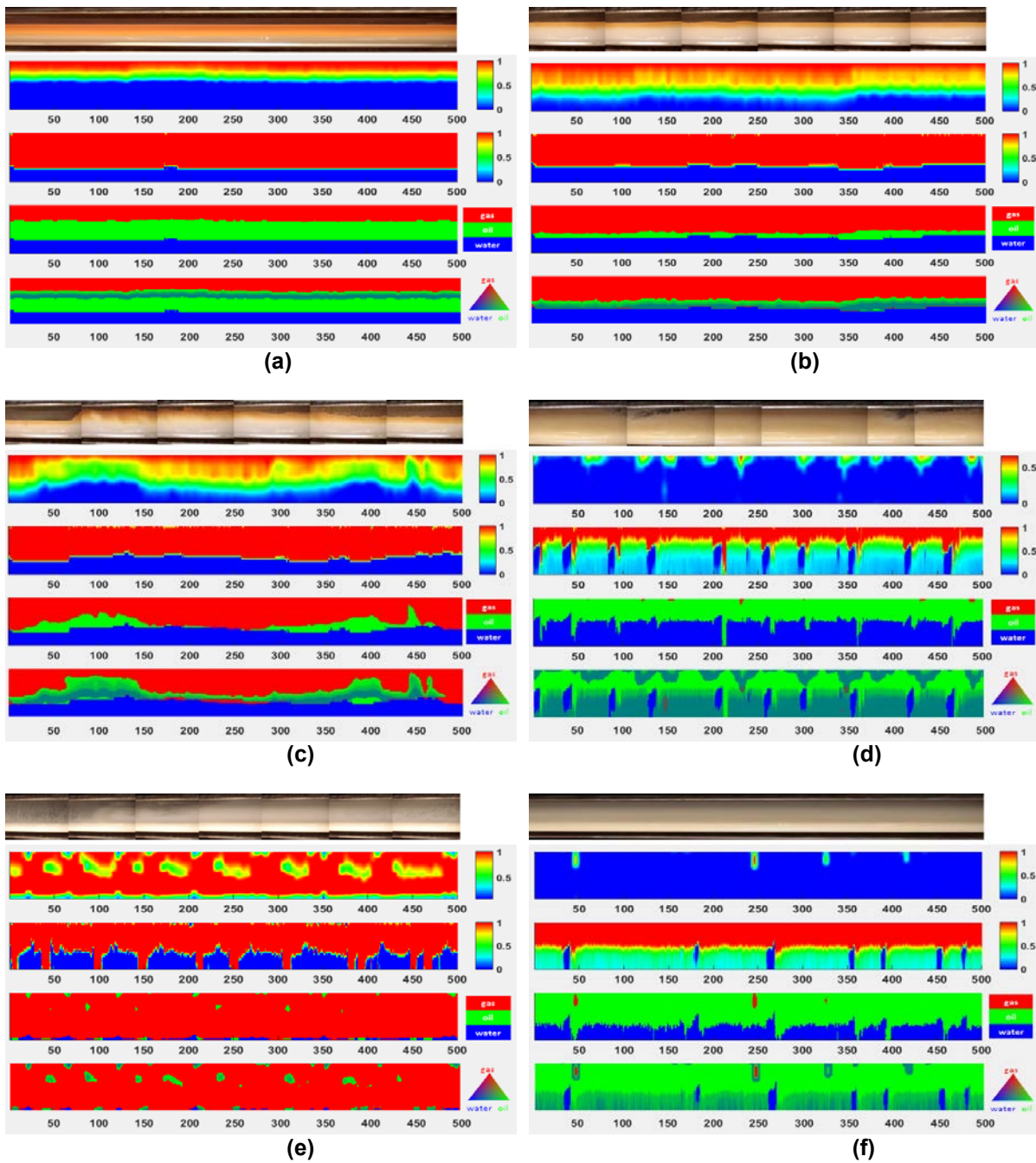


Figure 4: Axial stacked images from high-speed video (the first from the top to bottom in each image column), ECT (the second), ERT (the third), threshold-based fusion (the fourth), and fuzzy logic-based fusion (the fifth), for (a) stratified flow; (b) wavy stratified flow; (c) slug flow; (d) plug flow; (e) annular flow; and (f) bubbly flow.

Table 2: Mean concentrations of different flow regimes by conventional threshold-based method and the proposed approach.

	Stratified flow		Wavy stratified flow		Slug flow	
	Threshold	FIS	Threshold	FIS	Threshold	FIS
gas (%)	48.63	48.15	51.56	51.84	49.62	47.58
oil (%)	19.57	21.08	11.62	14.18	12.60	17.50
water (%)	31.80	30.77	36.82	33.97	37.78	34.92

	Plug flow		Annular flow		Bubbly flow	
	Threshold	FIS	Threshold	FIS	Threshold	FIS
gas (%)	2.84	5.92	91.54	93.72	10.99	0.97
oil (%)	30.05	58.38	1.90	4.06	35.66	74.27
water (%)	67.11	35.58	6.56	2.22	53.35	24.76

The results are depicted in Figure 4. For each flow regime, stacked images from high-speed camera and 4 axial cross-sectional images extracted from 500 consecutive frames of ECT, ERT, threshold-based fusion, and fuzzy logic-based fusion are presented together show their capability in visualisation of typical five flow patterns in horizontal flows. Table 2 lists the mean concentrations for all tested flow conditions by threshold-based method and the proposed approach.

From visual perspectives, the proposed approaches fused images are overall competitive with those by conventional threshold-based methods. As ECT and ERT are able to approximately identify the interface between each phase, e.g. in Figure 4b, FIS-based approach generates qualitative images very close to the ones by the thresholding method, despite some distortion close to phase interface. This, however, reflects the limitations of electrical tomographic system, e.g. blurred boundaries between gas and liquid. However, when either of the applied modalities is incapable of presenting good-quality tomograms, the FIS-based results are not as good as the ones by thresholding method, e.g. the bubbly flow in Figure 4f.

3.3 Impacts of selective parameters on performance

In order to evaluate the impacts of the parameters on both methods, different parameters are selected for each method. For each threshold, particular low-mid, mid-high, and high membership functions (MFs) are defined for both ECT and ERT input MFs, as specified in Table 3. The detailed definitions of the MFs can be found in Wang (2017).

Table 3: Different threshold values and membership functions.

Threshold	Low-mid MF	Mid-high MF	High MF
0.4	0.05 0.225 0.4	0.25 0.4 0.55	0.4 0.5 1.033 1.3
0.45	0.05 0.25 0.45	0.3 0.45 0.6	0.45 0.55 1.033 1.3
0.5	0.05 0.275 0.5	0.35 0.5 0.65	0.5 0.6 1.033 1.3
0.55	0.05 0.3 0.55	0.4 0.55 0.7	0.55 0.65 1.033 1.3

The first experiment was to change the ERT threshold values, including 0.4, 0.45, 0.5, 0.55, while kept the ECT threshold value at 0.5. The resultant mean concentrations of the phases for different ERT threshold values are listed in Table 4 from both threshold-based method and FIS-based method, and the images are demonstrated in Figure 5. Overall, both methods produce consistent results in terms of mean concentrations and images. In threshold-based method, the change of ERT threshold values have almost no effects to the mean concentrations of the phases, which is because the boundaries between water (the conductive phase) and gas and oil (the non-conductive phase) are sharp due to the application of sensitivity therron-based back-project (SBP). In contrast, in the FIS-based method, there is a tiny impact on the results with MFs change. The . From visualisation point of view, the integrated images are very similar except the boundaries between gas and oil in the FIS-based method are little blurred. This is primarily because of the blurred boundaries between gas and liquid in the original ECT images, which actually reflects the limitations of ECT tomograms in multiphase flow visualisation, as well as the nature of multiphase flow in terms of interfaces are usually mixed together.

Table 4: Mean concentrations.

ERT threshold	Threshold-base method			FIS-based method		
	Gas (%)	Oil (%)	Water (%)	Gas (%)	Oil (%)	Water (%)
0.4	32.53	40.62	26.85	33.28	41.05	25.66
0.45	32.53	40.62	26.85	33.28	40.84	25.87
0.5	32.53	40.62	26.85	33.28	40.70	26.02
0.55	32.53	40.61	25.86	33.28	40.57	26.14

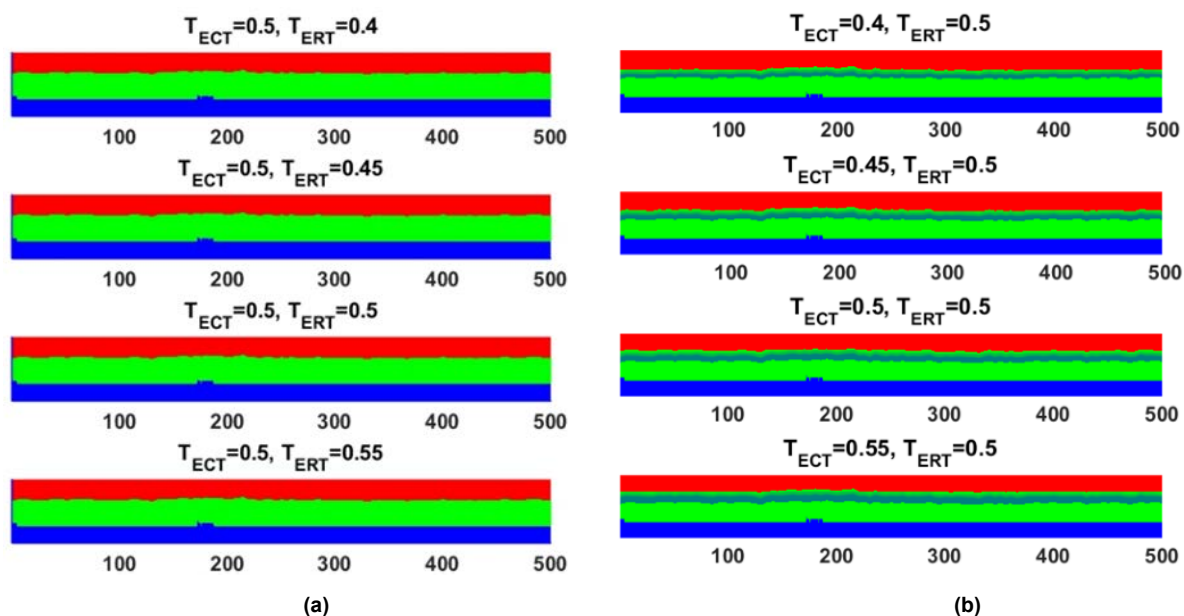


Figure 5: Images with same ECT threshold but different ERT thresholds by (a) conventional thresholding method; and (b) FIS-based approach.

The second experiment was to change the ECT threshold values, including 0.4, 0.45, 0.5, 0.55, while kept the ERT threshold value at 0.5. The derived mean concentrations are listed in Table 5, and the integrated tomograms are depicted in Figure 6. Table 5 shows that with the threshold increase, the gas concentration decreases, but the oil concentration increases. The gas concentration derived by the thresholding method declines a little faster than the one by the FIS-based method. From visualisation perspective, the results by both methods are very similar to the ones from the first experiment.

Table 5: Mean concentrations of each phase by different ECT thresholds for conventional method and different definitions of ECT membership functions for FIS-based approach.

ECT threshold	Threshold-base method			FIS-based method		
	Gas (%)	Oil (%)	Water (%)	Gas (%)	Oil (%)	Water (%)
0.4	35.54	37.60	26.86	35.57	38.41	26.02
0.45	33.81	39.33	26.86	34.55	39.43	26.02
0.5	32.53	40.62	26.86	33.28	40.70	26.02
0.55	31.23	41.92	26.85	32.12	41.86	26.02

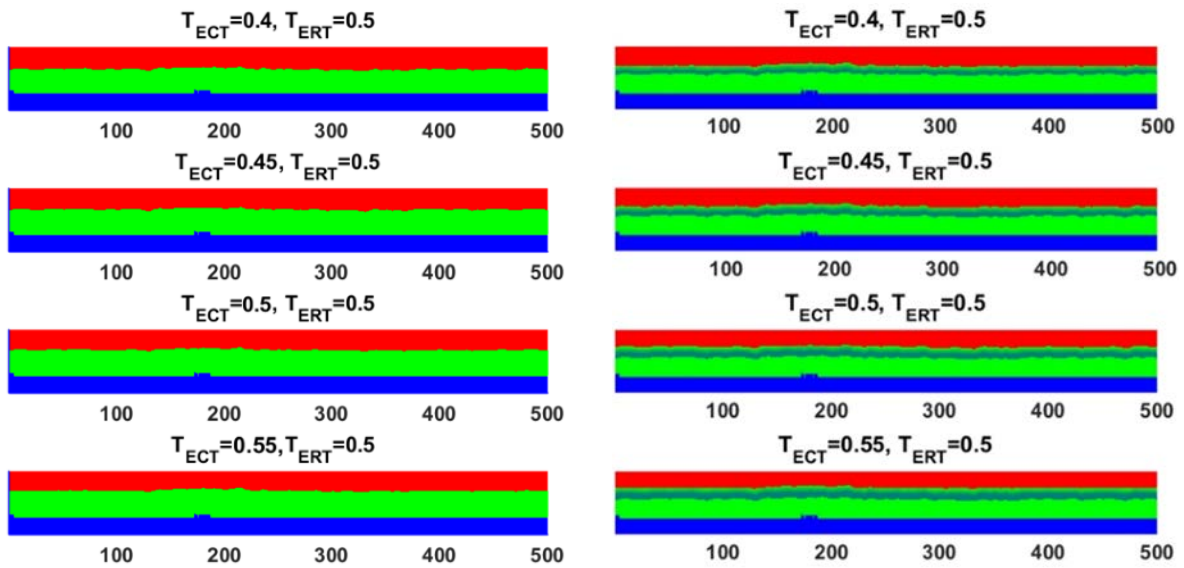


Figure 6: Images with different ECT thresholds but same ERT threshold by (a) conventional thresholding method; and (b) FIS-based approach.

4 CONCLUSIONS

Two different data fusion algorithms, i.e. threshold-based and fuzzy logic with decision tree-based algorithms, are introduced, and their performances on the six common flow regimes in a horizontal pipe are compared in the paper. The data from each modality containing different spatial and temporal information are fused successfully with both algorithms. However, due to the lack of local velocity information, the quantitative comparison was directly on the mean concentrations derived by both algorithms, rather than with reference values, e.g. gas volume fraction or water-liquid ratio.

Overall, the threshold-based approach is easy to be understood, simple to be implemented, and requires acceptable time and resources. Therefore, it is suitable for online purpose. However, its primary limitation is the determination of the threshold values, which usually requires a priori knowledge. As the values have considerable impacts on the fusion results, they have to be chosen with extreme care. In contrast, fuzzy logic with decision tree-based approach is theoretically complicated, and involves substantial amount of computation, and therefore is time and resource-expensive. On the other hand, it is insensitive to the changes of different membership functions, resulting in more stable outcomes in both qualitative and quantitative terms. However, it is worth noting that the latter approach is sensitive to the quality of the input data.

ACKNOWLEDGEMENTS

The authors appreciate the financial supports by the Engineering and Physical Sciences Research Council (EP/H023054/1), the European Metrology Research Programme (ENG58-MultiFlowMet) project Multiphase flow metrology in the Oil and Gas production, and the European Metrology Programme for Innovation and Research project (16ENG07-MultiFlowMet II) project multiphase flow reference metrology, which are jointly funded by the European Commission and participating countries within Euramet and the European Union.

REFERENCES

- HOYLE, B. S., JIA, X., PODD, F. J. W., SCHLABERG, H. I., TAN, H. S., WANG, M., R M WEST, R. A. W., AND YORK, T. A. (2001). Design and application of a multi-modal process tomography system. *Measurement Science and Technology*, 12(8):1157.
- HOYLE, B. S. AND WANG, M. (2012). Multi-dimensional opportunities and data fusion in industrial process tomography. *IEEE Instrumentation and Measurement Technology Conference (I2MTC)*, 2012, pages 916–920.
- MILLINGTON, D. (2016). Eng58 multiphase flow metrology in oil and gas production - work package 4 (flow visualisation). Technical report, TUV NEL.
- PUSPPANATHAN, J., FARAMARZI, M., YUNUS, F. R., AYOBR, N. M. N., RAHIM, R. A., PHANG, F. A., RAHIMAN, M. H. F., AHMAD, A., LING, L. P., AND ABAS, K. H. (2014). Image fusion using fuzzy logic pixel fusion for dual modality tomography system. *Jurnal Teknologi*, 70(3).
- QIU, C., HOYLE, B. S., AND PODD, F. J. W. (2007). Engineering and application of a dual-modality process tomography system. *Flow Measurement and Instrumentation*, 18(5-6):247 – 254. *Process Tomography and Flow Visualization*.
- SUN, J. AND YANG, W. (2015). A dual-modality electrical tomography sensor for measurement of gas-oil-water stratified flows. *Measurement*, 66:150 – 160.
- WANG M, (ed) (2015) *Industrial Tomography - Systems and Applications*, Elsevier, ISBN: 978-1-78242-118-4.
- WANG, Q. (2017). *A Data Fusion and Visualisation Platform for Multi-Phase Flow by Electrical Tomography*. PhD thesis, Univesrity of Leeds.
- WANG, Q., WANG, M., WEI, K., AND QIU, C. (2017). Visualization of gas-oil-water flow in horizontal pipeline using dual-modality electrical tomographic systems. *IEEE Sensors Journal*, 17(24):8146–8156.
- YUE, S., WU, T., PAN, J., AND WANG, H. (2013). Fuzzy clustering based et image fusion. *Inf. Fusion*, 14(4):487–497.